



**Proposal of an experimental test at DAΦNE for the low emittance muon beam production from positrons on target**

M. Boscolo, M. Antonelli, O.R. Blanco-García, S. Guiducci, A. Stella  
INFN-LNF, Via E. Fermi 40, 00044 Frascati, Rome, Italy  
S. Liuzzo, P. Raimondi  
ESRF, 71 avenue des Martyrs, 38000 Grenoble, France  
F. Collamati  
INFN-Rome, Piazzale A. Moro 2, 00185 Rome, Italy  
R. Li Voti  
La Sapienza University-Rome, Piazzale A. Moro 2, 00185 Rome, Italy

**Abstract**

We present in this paper the proposal of an experimental test at DAΦNE of the positron-ring-plus-target scheme foreseen in the Low EMittance Muon Accelerator. This test would be a validation of the on-going studies for LEMMA and it would be synergic with other proposals at DAΦNE after the SIDDHARTA run. We discuss the beam dynamics studies for different targets inserted in a proper location through the ring, i.e. where the beam is focused and dispersion-free. Optimization of beam parameters, thickness and material of target and optics of the target insertion are shown as well. The development of the existent diagnostic needed to test the behavior of the circulating beam is described together with the turn-by-turn measurement systems of charge, lifetime and transverse size. Measurements on the temperature and thermo-mechanical stress on the target are also under study.

## 1 Introduction

We believe that the dynamics of a beam affected by the turn-by-turn interaction with a target while circulating in a storage ring can be of interest for different point of views. Such a study can be performed at the DAΦNE low energy storage ring. In this respect, measurements would be a benchmark for the simulation studies and a validation of the positron–ring–plus–target scheme foreseen in LEMMA.

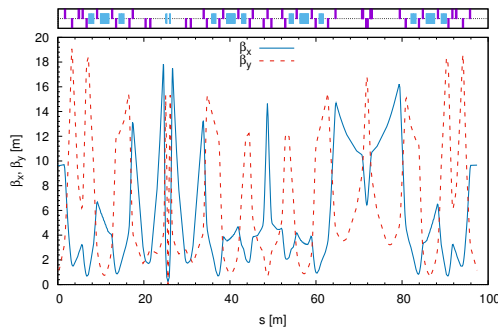


Figure 1:  $\beta$  functions of the SIDDHARTA 2009 optics. The thin target is placed at the Interaction Point at  $s=25.607$  m in the plot.

Beam dynamics and target thermo-mechanical issues can be studied at DAΦNE even if the beam energy is as low as 0.51 GeV and large differences in many important parameters are present. DAΦNE will end its collider operation at the end of 2019 with the SIDDHARTA-2 experiment, we propose this test at the end of this run, using either the electron or the positron beam. The beam lifetime and beam size evolution can be measured and compared with numerical predictions performed specifically for DAΦNE with the same tools used for the LEMMA design study. Measurements of the beam size perturbations dependence on the optical parameters can be performed, together with experimental studies on the target issues related to heat load and thermo-mechanical stress. Different thicknesses and materials of the target can also be tested. Given the limited energy acceptance of the ring, we plan to test Be or C targets with thicknesses in the range of 10-100  $\mu\text{m}$ . Also crystal channeling can be envisaged.

## 2 Optics and Beam Dynamics simulations

We present here first beam dynamics studies with the SIDDHARTA 2008-2009 optics, more detailed simulations are needed for the preparatory phase of the test. To minimize the cost of this experiment we propose to use the existing configuration with only minimal modifications needed to insert a target and diagnostics. The target is placed at the Interaction Point (IP), where the low- $\beta$  functions and zero dispersion allow the suppression of multiple scattering and Bremstrahlung effects.

Beta functions are shown in Figure 1, the IP is at  $s=25.607$  m in the plot and corresponds to the longitudinal location of the target. Here the beam spot size is  $\sigma_x = 0.27$  mm

Table 1: DAFNE parameters for the test with thin target at IP.

Parameter	Units	
Energy	GeV	0.51
Circumference	m	97.422
Coupling(full current)	%	1
Emittance x	m	$0.28 \times 10^{-6}$
Emittance y	m	$0.21 \times 10^{-8}$
Bunch length	mm	15
Beam current	mA	5
Number of bunches	#	1
RF frequency	MHz	368.366
RF voltage	kV	150
N. particles/bunch	#	$1 \times 10^{10}$
Horizontal Transverse damping time	ms/turns	42 / 120000
Vertical Transverse damping time	ms/turns	37 / 110000
Longitudinal damping time	ms/turns	17.5 / 57000
Energy loss/turn	keV	9
Momentum compaction		$1.9 \times 10^{-2}$
RF acceptance	%	$\pm 1$

and  $\sigma_y = 4.4 \mu\text{m}$ , resulting from the beta functions at IP of  $\beta_x^*=26 \text{ cm}$  and  $\beta_y^*=0.9 \text{ cm}$  and horizontal emittance of  $0.28 \times 10^{-6} \text{ m}$ . The main parameters needed for this test are summarised in Table 1.

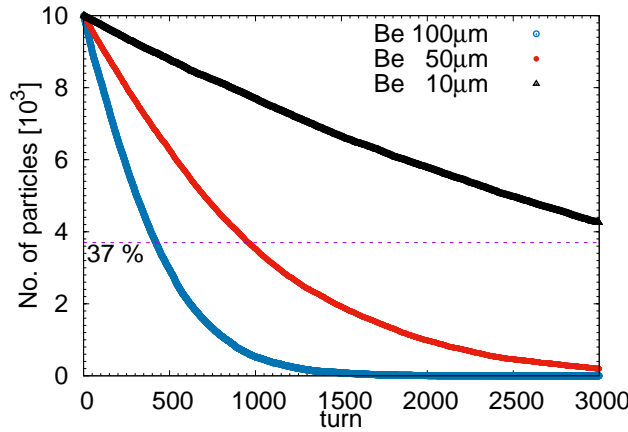


Figure 2: Number of  $e^+$  vs number of machine turns with a 10, 50 and 100  $\mu\text{m}$  Be target at the IP. The 37% line indicates the resulting beam lifetime in terms of turns.

Particle tracking in the ring is performed using PTC MAD-X and GEANT4, as for the 45 GeV LEMMA ring. The resulting energy acceptance with this optics configuration is 1%.

Figure 2 shows the number of particles as a function of machine turns for a Be target of different thicknesses: 10, 50 and 100  $\mu\text{m}$ . The 37% line indicates the resulting beam lifetime in terms of turns. Lifetime of about 4000 turns is found for 10  $\mu\text{m}$  thick Be target,

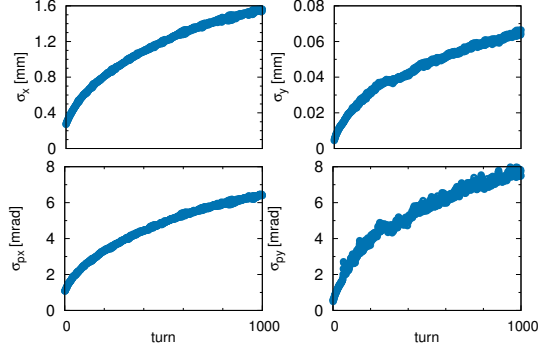


Figure 3: Evolution of horizontal and vertical beam size and divergence for a Be target of  $50 \mu\text{m}$ .

about 1000 turns for  $50 \mu\text{m}$  and 500 turns for  $100 \mu\text{m}$ .

The evolution of the transverse beam size and divergence with the number of turns for  $50 \mu\text{m}$  Be target is shown in Figure 3.

Figure 4 shows the 6D phase-space before the interaction with the target and after 900 turns for a  $50 \mu\text{m}$  Be target in the ring.

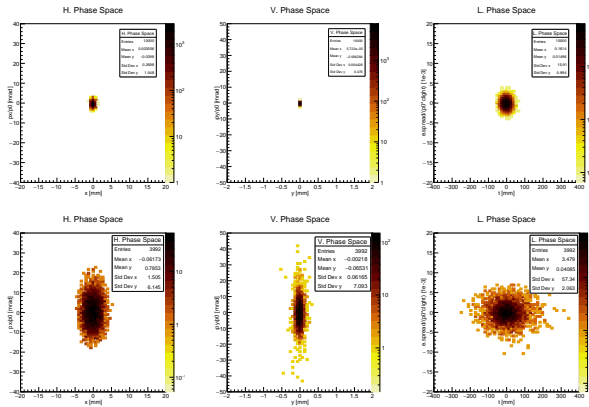


Figure 4: 6D phase space at the target at the first machine turn and after 900 turns with a  $50 \mu\text{m}$  Be target.

### 3 Experimental set-up

Beam measurements of charge, lifetime and transverse size in the DAΦNE storage ring are essential to achieve a beam characterization after interaction with the target. To cope with the beam parameters required for this test (Table 1) and given the perturbation of the target, which will not allow to store the beam in the ring, some modifications to the existing beam diagnostics will be required.

During the usual collider operation, measurements of the average stored beam current is available, with resolution better than 0.1%, through acquisition of toroidal DC current monitors signals installed in each ring. The available bandwidth of this specific pickup can provide accurate average beam current measurements only for a beam lifetime

as short as  $100\mu\text{s}$ . When needed in this test, real turn by turn beam charge measurements (with resolution in the order of 1%) will be also available through sampling of common mode signals from beam position monitors installed along the rings. By using a pre-existing hardware included in the DAΦNE orbit system, after proper reconfiguration of timing and development of software acquisition tools, it will be possible to sample up to 64 kTurns ( $\sim 20$  ms) after each bunch injection.

A dedicated synchrotron radiation line, collecting synchrotron radiation in the visible wavelength range emitted from the beam passing in one of the dipole magnets, is routinely used during DAΦNE collider operation to measure the transverse and longitudinal size of the stored beam by imaging. Given the radiation source in a zone with vanishing value of the dispersion function, the beam transverse emittances can be directly evaluated from horizontal and vertical dimension measurements. A beam transverse size measurement system at each turn in the ring can be implemented with dedicated modifications of the existing optic equipment and instrumentation. By taking advantage of the gating capabilities of a CCD gated camera with image intensifier (already operating in the DAΦNE instrumentation) the synchrotron radiation beam image will be focused in the CCD camera sensor at revolution time intervals and averaged over subsequent injection to increase signal to noise ratio. The beam size enlargement (Figure 4) and the beam charge foreseen for this test (Table 1) appears to be compatible with the actual system aperture and sensitivity.

#### **4 Temperature measurement in situ on the target**

A robust experimental setup should be designed for measuring contactless the temperature of the target surface at the microsecond scale and with a high spatial resolution ( $10\mu\text{m}$ ). Several technical solutions can be adopted by using different measurement techniques.

##### **4.1 Passive Infrared thermography**

It is a remote sensing technique. The infrared camera works outside the vacuum chamber and can detect the IR emission of the hot target through a transparent IR window (for example CaF window). Since the maximum temperature of the target is expected in the range  $500^{\circ}\text{C}$ – $1000^{\circ}\text{C}$ , according to the Planck law, the InSb cameras working in the MIR spectral band  $3\text{--}5\mu\text{m}$  can give optimal performances. For example in Figure 5 it is reported the thermal image of the cross section of three layered polyamide films [15]. The InSb camera has  $256 \times 256$  pixels showing a very good spatial resolution  $7.5\mu\text{m}$  ( $3\mu\text{m}/\text{pixel}$ ). The frame rate can vary from 60 Hz to 5000 Hz, corresponding to the pixel size  $256 \times 256 \sim 64 \times 64$ . This means that the time resolution can be obtained by loosing the spatial resolution.

One disadvantage is that the IR camera is not fast enough to follow the dynamic range of the temperature in  $\mu\text{s}$  range. Nevertheless the cooling dynamic after the pulse can

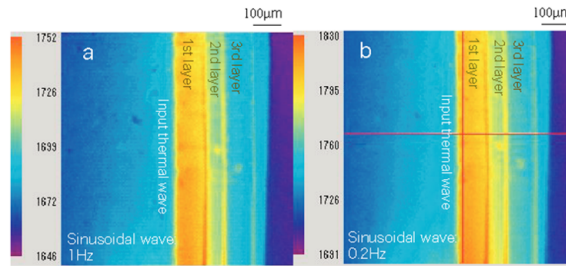


Figure 5: Example of spatial resolution obtainable with an InSb infrared camera on 3 thin layers [15].

be clearly measured so that the maximum temperature during the pulse can be extrapolated according to the known geometry (see some examples on the extrapolation [17,18]).

## 4.2 Infrared radiometry

This is also a remote sensing technique. The infrared detection system works outside the vacuum chamber and, after calibration, can monitor the temperature in one point (the hottest region i.e. the center of the pulse) from the IR emitted by the target. Even in this case the HgZnCdTe infrared detector should have the best performances in the spectral band  $2-5\mu\text{m}$ . The advantage in this case is that the detector can be pretty fast following the temperature dynamics in the microsecond range. The disadvantage is that one can monitor the temperature in one point only (see ref[19]).

## 4.3 Measurement of surface deformation of the target and temperature determination

A contactless measurement of the surface deformation can be performed with laser technique as shown in Fig.6. The target is subject to a surface thermoelastic deformation induced by the heat deposition. The maximum deformation is expected at the centre of the pulse. The probe laser beam enters the vacuum chamber and is reflected back by the target surface. When the target surface is subjected to a thermoelastic deformation the probe beam changes its direction of reflection. This change is measured by a position sensor. This technique is very sensitive and can detect very weak deformation of the order of some picometer corresponding to less than  $1^\circ\text{C}$ . After a proper calibration it can be used to follow the ultrafast dynamic of the temperature of the target (see ref.[20,21])

## References

- [1] Muon Accelerator Program web page: <http://map.fnal.gov>
- [2] M.A. Palmer, "The US muon accelerator program", TUPME012, IPAC' 14, Dresden, Germany (2014).

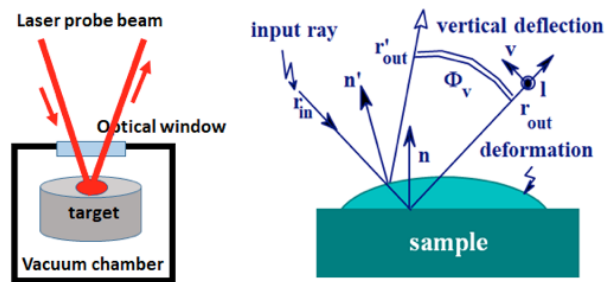


Figure 6: Surface deformation measurements.

- [3] M. Antonelli, M. Boscolo, R. Di Nardo and P. Raimondi, “Novel proposal for a low emittance muon beam using positron beam on target,” Nucl. Instrum. Meth. A **807** (2016) 101 doi:10.1016/j.nima.2015.10.097
- [4] M. Antonelli, E. Bagli, M. Biagini, M. Boscolo, G. Cavoto, P. Raimondi and A. Variola, “Very Low Emittance Muon Beam using Positron Beam on Target,” TUPMY001, IPAC’16, Busan, Korea (2016).
- [5] W. A. Barletta and A. M. Sessler, “Characteristics of a high-energy  $\mu^+\mu^-$  collider based on electroproduction of muons”, Nucl. Instrum. Meth. A **350** (1994) 36.
- [6] R. Chehab, “Angular collection using solenoids”, Nucl. Instrum. Meth. A **451** (2000) 362-366.
- [7] B. Nash *et al.*, “New Functionality for Beam Dynamics in Accelerator Toolbox (AT)”, MOPWA014, IPAC’15, Richmond, VA, USA (2015).
- [8] MAD-X web page: <http://madx.web.cern.ch/madx/>; E. Forest and F. Schmidt, PTC - User Reference Manual (2010).
- [9] S. Agostinelli, et al., “GEANT4: A Simulation toolkit”, Nucl. Instrum. Meth. A **506** (2003) 250–303.
- [10] A. Ferrari, P. R. Sala, A. Fasso and J. Ranft, “FLUKA: A multi-particle transport code (Program version 2005),” CERN-2005-010, SLAC-R-773, INFN-TC-05-11.
- [11] S. Halfon *et al.*, “High-power liquid-lithium jet target for neutron production,” Rev. Sci. Instrum. **84** (2013) 123507.
- [12] see for example: D. J. Summers, “Muon acceleration using fixed field, alternating gradient (FFAG) rings,” Int. J. Mod. Phys. A **20** (2005) 3861
- [13] Y. Alexahin, “Design of muon collider lattices,” NA-PAC2016, USA (2016).
- [14] M-H. Wang, Y. Nosochkov, Y. Cai and M. Palmer, “Design of a 6 TeV Muon Collider”, SLAC-PUB-16249 (2015)

- [15] J. Morikawa, T. Hashimoto, E. Hayakawa, T. Eto, and R. Li Voti, "Thermal characterization of multi-layer polymer films by IR thermography", Proceedings of QIRT 8th Conference (2006)
- [16] M. C. Larciprete, A. Albertoni, A. Belardini, G. Leahu, R. Li Voti, F. Mura, C. Sibilìa, I. Nefedov, I. V. Anoshkin, E. I. Kauppinen, A. G. Nasibulin, "Infrared properties of randomly oriented silver nanowires" JOURNAL OF APPLIED PHYSICS (ISSN:0021-8979), 083503-1- 083503-6, (2012).
- [17] M.Bertolotti, G. Liakhov , R. Li Voti, C. Sibilìa, A. Syrbu, R.P.Wang, "New method for the study of mirror heating of a semiconductor laser diode and for the determination of thermal diffusivity of the entire structure" Appl. Phys. Lett. 65 (18), p.2266 (1994).
- [18] M.Bertolotti, G.L.Liakhov, R.Li Voti, R.P.Wang, C.Sibilìa, A.V.Syrbu and V.P.Yakovlev, "An experimental and theoretical analysis of the temperature profile in semiconductor laser diodes using the photodeflection technique", Meas. Sci. Technol. 6, p.1278 (1995).
- [19] G. Leahu, R. Li Voti, C. Sibilìa, M. Bertolotti, Applied Physics Letters, 103 (23), 231114 (2013).
- [20] M.Bertolotti, R.Li Voti, S.Paoloni, C.Sibilìa, G.L.Liakhov, "Analysis of the photothermal deflection method in the bouncing scheme", Progress in Natural Science Suppl.Vol.6 p.665 (1996).
- [21] M.Bertolotti, R.Li Voti, S.Paoloni, C.Sibilìa, G.L.Liakhov, "Temperature measurement by optical beam deflection method", Proceedings from 6th International Symposium on Temperature and Thermal Measurements in Industry and Science (TEMPMEKO '96), Torino, p.421 (1996).
- [22] M.Bertolotti, R.Li Voti, S.Paoloni, C.Sibilìa, G.L.Liakhov, "Surface deformation measurement by photothermal deflection technique", SPIE Vol. 2782 from Optical Inspection and Micromasurements, p.504 (1996).
- [23] M.Bertolotti, G.L.Liakhov, R.Li Voti, S.Paoloni, C.Sibilìa, "Analysis of the photothermal deflection technique in the surface reflection scheme: Theory and experiment" - J.Appl.Phys 83 (2) 1998 p.966-982.
- [24] M. Tomoda, O. B. Wright, R. Li Voti, "Nanoscale thermoelastic probing of megahertz thermal diffusion", Appl. Phys. Lett. 91, 071911 (2007)